representing at least 47 min, and hence variables representing at least 62 min, of potential demand must remain unserviced. The constraint

$$22\chi_3+15(\chi_5+\chi_6)+25\chi_{14}+45\chi_{47} \geqq 62$$

will clearly cause this.

Another common constraint arises because two or more variables may in fact represent alternative allocations which would satisfy a single need. Satellite 1234 has already been assigned variables χ_5 and χ_6 at station C. It may be that a pass an hour later at station A would also satisfy the sponsor's communication need and that this pass has been assigned variable χ_{251}. Since multiple contacts would be wasteful of the SCN resources and the satellite's energy capacity, a constraint is introduced to ensure that at most one of the alternatives is used. This means at least two must remain unused, or that

$$\chi_5+\chi_6+\chi_{251} \geqq 2$$

Many other system constraints and logical situations can be represented within the 0-1 LP, paradigm, including various logical implications. A user quickly becomes familiar with the possibilities once he learns the basic ones above. Care must be exercised, however, to avoid creating contradictory constraints which require a variable to simultaneously take on the values zero and one. This is best avoided by using constraints only to keep resources from being overburdened and not to force passes to be serviced.

III. Preliminary Resource Allocation Program

In order to experiment with the above approach, a limited resource allocation program called RAP was programed to run on a CDC 6600 computer. A fully operational allocation program reflecting the entire potential of 0-1 LP will take a large effort and considerable further research to develop. The limited version, nevertheless, provides useful insight into the nature of the SCN problem, and for this reason its properties are considered in the following paragraphs.

The computational flow of RAP is very simple and is essentially that of Fig. 1. A Geoffrion algorithm[8] is used for the 0-1 LP optimization. RAP is a study program rather than a production program, but certain of its characteristics are worth examining.

1) The program is written entirely in FORTRAN for CDC 6600/7600 computers. It requires about 3500 cards, and the instructions use about 6000 words of memory. No auxiliary storage is used. The program fills core for large problems unless the matrices, which tend to be sparse, are packed.

2) Running time depends upon both problem size and the character of the constraints. Many problems have been solved using only a single pass through the standard simplex algorithm utilized by the Geoffrion 0-1 LP algorithm. In such cases scenarios involving 500 passes yielding 800 0-1 variables have been processed in less than two minutes of CPU time.

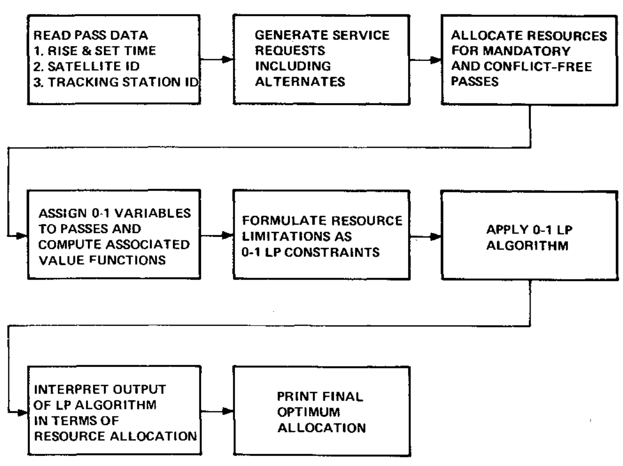

Fig. 1 Processing flow of RAP program for SCN resource allocation.

3) It has been difficult to compare the automated schedule directly with that produced by a human. A small scenario processed by RAP proved impossible for a human to improve. In real scheduling, however, human schedulers are allowed to bend rules which the computer presently treats as inviolate.

The limited experience achieved so far with this program along with discussions with potential users of such a system have indicated that the method has significant potential for performing system studies and as an aid in planning real schedules. Its ability to always produce an optimum within its ground rules will lend credibility to such tradeoff studies as the cost/benefits of deleting or improving resources and will remove much tedious detail from real scheduling exercises.

The experience and discussions have also revealed that advanced versions of RAP would need certain improvements. Larger scenarios must be handled, and decisions concerning scheduling of communications with high-altitude satellites, which have long visibility intervals, can probably be made more efficiently than by RAP's method of discretizing the intervals into a small number for which "yes-no" decisions are made. Furthermore, the previous comment (3) indicates that the program should either be modified to do some "rule-bending" or it should be run in an interactive mode.

References

[1] Ellis, W. and Lenske, M. D., "Scheduling and Control of Satellite Communication Systems," *Communications Satellite Systems Technology*, Academic Press, New York, 1966, pp. 755–774.

[2] Driscoll, L. C. and Suyemoto, L., "Heuristics for Resolution of Logical Scheduling Conflicts," MTR-157, Oct. 1966, Mitre Corp., Bedford, Mass.

[3] Brewer, A. C., "Interactive Scheduling System," *IBM Systems Journal*, No. 1, 1971, pp. 67–79.

[4] Wagner, H. M., *Principles of Operations Research*, Prentice-Hall, Englewood Cliffs, N.J., 1969, Chap. 13.

[5] Conway, R. W., Maxwell, W. L., and Miller, L. W., *Theory of Scheduling*, Addison-Wesley, Reading, Mass., 1967.

[6] Downs, H. R. and Wishner, R. P., "Scheduling Cars in a People Moving System," *Proceedings of the Fifth Hawaii International Conference on Systems Sciences*, University of Hawaii, Honolulu, Hawaii, 1972, pp. 561–563.

[7] Pritsher, A. A. B., Watters, L. J., and Wolf, P. M., "Multiproject Scheduling with Limited Resources: A Zero-one Programing Approach," P-3800, Feb. 1968, Rand Corp., Santa Monica, Calif.

[8] Geoffrion, A. M., "An Improved Implicit Enumeration Approach for Integer Programing," *Operations Research*, Vol. 17, No. 3, 1969, pp. 437–454.

Effect of Transverse Products of Inertia on Re-Entry Vehicle Trim Angle Behavior

ALBERT E. HODAPP JR.*
Sandia Laboratories, Albuquerque, N. Mex.

Nomenclature

c.g. = center of gravity
C_A = axial force coefficient

Received March 29, 1974; revision received May 9, 1974. This work was supported by the U.S. Atomic Energy Commission. The author wishes to thank G. E. Reis, J. R. Kelsey, and G. G. Wilson of Sandia Laboratories for their assistance and suggestions.

Index categories: Entry Vehicle Dynamics and Control; LV/M Dynamics and Control.

* Member of the Technical Staff, Aerodynamics Projects Department. Member AIAA.

C_{m_o} = aerodynamic asymmetry induced pitching moment coefficient
$C_{m_q}+C_{m_{\dot\alpha}}$ = damping derivative coefficients (based on $d/2U$), 1/rad
C_{m_α} = pitching moment slope coefficient, 1/rad
C_{n_o} = aerodynamic asymmetry induced yawing moment coefficient
C_{N_α} = normal force slope coefficient, 1/rad
d = vehicle base diameter (reference length), ft or m
i = $(-1)^{1/2}$
I, I_X = lateral and axial moments of inertia, respectively, slug-ft^2 or kg-m^2
J_{XY}, J_{YZ}, J_{XZ} = products of inertia relative to X, Y, Z axes, slug-ft^2 or kg-m^2
m = vehicle mass, slug or kg
p, p_{cr} = roll rate and critical roll rate, respectively, rad/sec
q' = dynamic pressure, lb/ft^2 or N/m^2
S = reference area, ft^2 or m^2
t = time, sec
U = total velocity, fps or m/sec
X, Y, Z = body reference axes, mutually parallel to X_g, Y_g, Z_g axes, with origin at the c.g. (Fig. 1)
X_g, Y_g, Z_g = geometric axes, with X_g the axis of geometric symmetry (Fig. 1)
X_p, Y_p, Z_p = principal axes (Fig. 1)
$y_{c.g.}, z_{c.g.}$ = position of the c.g. relative to origin of X_g, Y_g, Z_g axes along Y_g and Z_g axes (Fig. 1), ft or m
α_T, β_T = trim angle of attack and trim angle of sideslip, respectively, rad or deg
$(\dot{\ })$ = first derivative with respect to time

Introduction

IN Ref. 1 a small angle quasi-steady analytical theory was presented describing the effects of unsymmetrical aerodynamic stability derivative characteristics and transverse products of inertia on the trim angle behavior of slender rolling re-entry vehicles. A discussion of the effects of unsymmetrical stability derivatives was given in Ref. 1; the effects of transverse products of inertia are discussed in this Note. Like unsymmetrical stability derivative characteristics, but to a much lesser degree, transverse products of inertia change the trim magnification near resonance and alter the windward meridian behavior. It is shown in this Note that when trim-producing asymmetries are present, the transverse product of inertia can increase or decrease the instability in re-entry vehicle trim angle behavior near resonance encounters. These results should be of interest because the effects of transverse products of inertia have been ignored in past trim angle analyses (Ref. 2 is representative), and because spin balancing of a vehicle about a longitudinal axis does not cancel this product of inertia.

Results and Discussion

The effects of the transverse J_{YZ} product of inertia on trim angle behavior are investigated herein by assuming that the lateral moents of inertia and stability derivative characteristics of the re-entry vehicle are symmetrical. With these assumptions, Eqs. (5) and (6) of Ref. 1 reduce to

$$\alpha_T = \frac{(\alpha_{T_R}-\delta_\alpha\lambda^2)(1-\lambda^2)-\lambda(\beta_{T_R}-\delta_\beta\lambda^2)(\mu+\lambda\delta_{YZ})}{(1-\lambda^2)^2+\lambda^2\mu^2-\lambda^4\delta_{YZ}^2} \tag{1}$$

and

$$\beta_T = \frac{(\beta_{T_R}-\delta_\beta\lambda^2)(1-\lambda^2)+\lambda(\alpha_{T_R}-\delta_\alpha\lambda^2)(\mu-\lambda\delta_{YZ})}{(1-\lambda^2)^2+\lambda^2\mu^2-\lambda^4\delta_{YZ}^2} \tag{2}$$

where

$$\lambda = p/p_{cr}$$

$$p_{cr} = \pm[-C_{m_\alpha}q'Sd/(I-I_X)]^{1/2}$$

$$\mu = \pm\left\{\frac{-\rho^{1/2}S\left[\dfrac{1}{2m}(C_A-C_{N_\alpha})+\dfrac{d^2}{4}\left(\dfrac{C_{m_q}+C_{m_{\dot\alpha}}}{I-I_X}\right)\right]}{[-C_{m_\alpha}Sd/2(I-I_X)]^{1/2}}\right\}$$

$$\delta_{YZ} = J_{YZ}/(I-I_X),\quad \delta_\alpha = J_{XZ}/(I-I_X),\quad \delta_\beta = J_{XY}/(I-I_X)$$

$$\alpha_{T_R} = \frac{-C_{m_o}}{C_{m_\alpha}} - \frac{C_A}{C_{m_\alpha}}\left(\frac{z_{c.g.}}{d}\right),\quad\text{and}\quad \beta_{T_R} = \frac{C_{n_o}}{C_{m_\alpha}} - \frac{C_A}{C_{m_\alpha}}\left(\frac{y_{c.g.}}{d}\right)$$

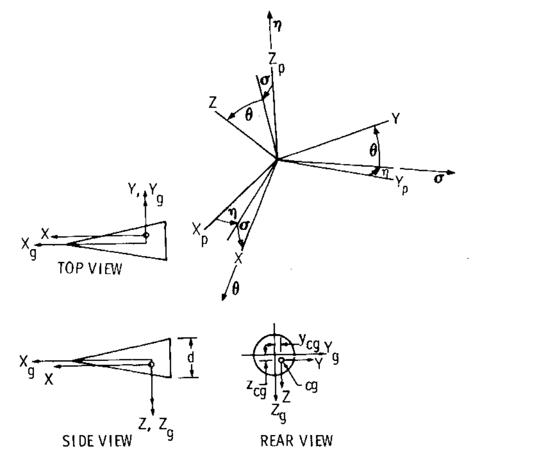

Fig. 1 Coordinate systems and nomenclature.

The quantities α_{T_R} and β_{T_R} are the reference trim angles which result from mass and aerodynamic asymmetry; δ_α and δ_β are the reference trim angles which result from inertia asymmetry.[2] The signs of p_{cr} and μ are the same as that of p. The roll rate ratio λ is always positive.

The reference coordinate system for Eqs. (1) and (2) is the XYZ body fixed axis system shown in Fig. 1. The angles η, σ, θ (Fig. 1) define the position of the XYZ body fixed axes relative to the $X_pY_pZ_p$ principal axes. When J_{YZ} is nonzero and the lateral moments of inertia are equal, $\theta = \pm\pi/4$ rad, $\sigma = (\delta_\alpha \mp \delta_\beta)/(1\mp\delta_{YZ})$ rad, and $\eta = -(\delta_\beta \pm \delta_\alpha)/(1\pm\delta_{YZ})$ rad. The upper of the double signs is used when $J_{YZ} > 0$, and conversely.

The behavior of the magnitude $|\zeta_T|$ and orientation ϕ of the total trim angle ζ_T will be investigated by varying λ while holding μ and δ_{YZ} constant. The total trim angle of attack may be defined in terms of α_T and β_T [Eqs. (1) and (2)] as follows:

$$\zeta_T = |\zeta_T|(\sin\phi + i\cos\phi) = \beta_T + i\alpha_T$$

where

$$|\zeta_T| = (\beta_T{}^2+\alpha_T{}^2)^{1/2},\quad\text{and}\quad \phi = \tan^{-1}(\beta_T/\alpha_T)$$

With the exception of Ref. 1, previous descriptions of re-entry vehicle trim angle behavior require only that the damping ratio μ be nonzero for trim magnification to remain finite. The presence of δ_{YZ} in the denominators of Eqs. (1) and (2) makes it possible for zeros to occur when μ is nonzero; therefore, α_T and β_T, and hence $|\zeta_T|$, can become unbounded. The denominator of $|\zeta_T|$, which is identical to those of Eqs. (1) and (2), is quadratic in λ^2. To find the values of λ which cause $|\zeta_T|$ to become undefined, the denominator is set equal to zero and the resulting

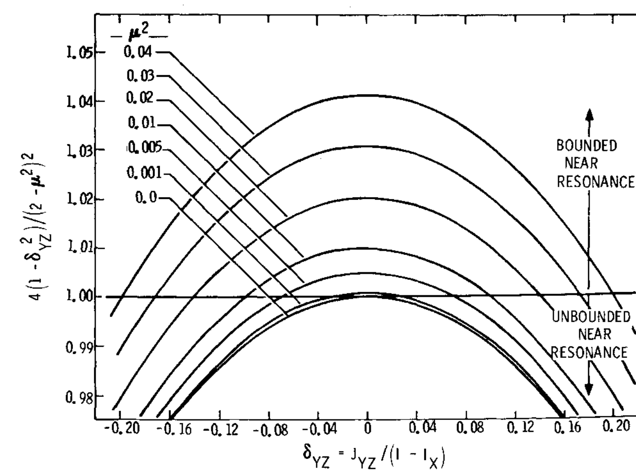

Fig. 2 Influence of transverse product of inertia on trim angle bounds.

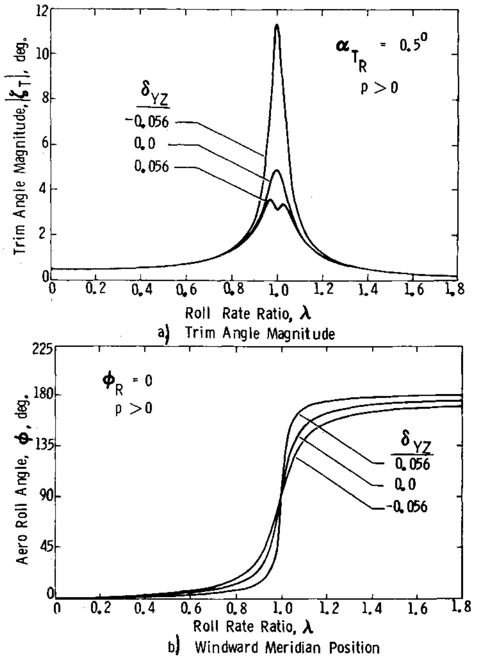

Fig. 3 Low altitude trim angle response with transverse product of inertia and mass and/or aerodynamic asymmetry.

biquadratic equation is solved for its roots. When positive real roots exist, they must satisfy

$$\lambda = \left[\frac{(2-\mu^2)}{2(1-\delta_{YZ}^2)}\right]^{1/2}\left\{1 \pm \left[1 - \frac{4(1-\delta_{YZ}^2)}{(2-\mu^2)^2}\right]^{1/2}\right\}^{1/2} \tag{3}$$

This equation indicates that when

$$4(1-\delta_{YZ}^2)/(2-\mu^2)^2 \leqq 1 \tag{4}$$

the roots are real, and therefore zeroes can occur in the denominator of $|\zeta_T|$ at positive real values of λ. For re-entry vehicles, these zeroes occur very close to the undamped resonance $\lambda = 1$. When $\delta_{YZ} = \mu$ and for certain reference trim conditions, zeroes can occur simultaneously in the numerators and denominators of Eqs. (1) and (2). Using L'Hospital's rule, it can be shown that α_T and/or β_T remain bounded for this condition.

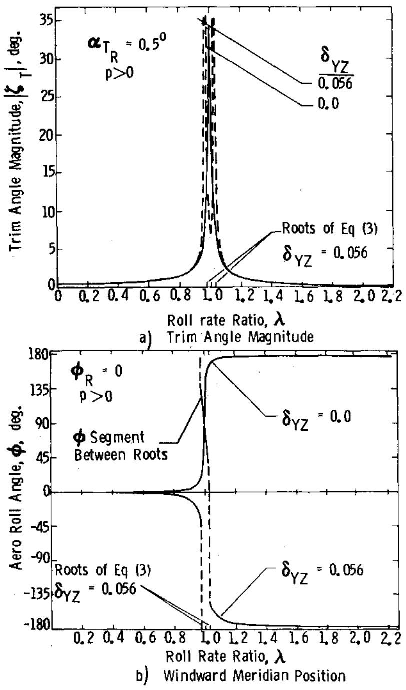

Fig. 4 High altitude trim angle response with transverse product of inertia and mass and/or aerodynamic asymmetry.

As shown in Fig. 2, the damping ratio μ has a strong influence on the range of δ_{YZ} over which the trim angle magnitude remains bounded near resonance. According to Eq. (4), the horizontal line on the figure separates the regions of bounded (imaginary λ above the line) and unbounded (positive real λ at and below the line) trim angles. The range of δ_{YZ} over which the trim angle remains bounded with varying λ is defined by the distance along the horizontal line between intersections of a μ^2 = const curve. As the damping ratio μ increases with decreasing altitude the range of δ_{YZ} for a bounded trim angle near resonance increases.

Some effects that the J_{YZ} product of inertia has on the trim angle behavior of a slender conical re-entry vehicle are shown in Figs. 3 and 4. The trim angle behavior patterns are representative of low altitude and high altitude resonance encounters for near maximum values of δ_{YZ} (bounds on δ_{YZ} for slender vehicles are ± 0.056). The $\delta_{YZ} = 0$ curves in Figs. 3 and 4 are the reference curves since they describe trim angle behavior that is not influenced by J_{YZ}. As shown in Figs. 3 and 4, the largest effects of δ_{YZ} on trim angle behavior occur near the undamped resonance.

Near resonance, the magnitude of the total trim angle $|\zeta_T|$ can be increased or decreased relative to the $\delta_{YZ} = 0$ reference curve by varying the sign and magnitude of δ_{YZ} (Fig. 3a). When the magnitude of δ_{YZ} satisfies Eq. (4), independent of the sign, an unbounded trim angle results (Fig. 4a). For the bounds $\delta_{YZ} = \pm 0.056$, unbounded trim angle magnitude can occur only for high altitude resonance encounters.

At the low altitude condition where δ_{YZ} is small enough for $|\zeta_T|$ to remain bounded, the windward meridian behavior (Fig. 3b) differs from that of the reference vehicle ($\delta_{YZ} = 0$) principally in the slopes of the ϕ vs λ curves near resonance and in the asymptotic value of ϕ as $\lambda \to \infty$. At the high altitude condition (Fig. 4b), in addition to the abovementioned differences, the windward meridian rotation direction can reverse (Fig. 4b) and between discontinuities in $|\zeta_T|$ [positive real roots of Eq. (3)], ϕ is biased 180°.

When the inertial coupling between the pitching-yawing and rolling motions provided by J_{YZ}

$$\dot{p} \approx (J_{YZ}/I_X)p^2\,|\zeta_T|^2 \cos 2\phi \tag{5}$$

is large, the rapid variations in λ which occur near resonance invalidate the theoretical assumptions thereby making it difficult to compare the theoretically predicted quasi-steady trim angle behavior with the trim angle behavior obtained from six-degree-of-freedom (6-DOF) numerical simulations. Where valid comparisons could be made, the 6-DOF results confirmed the theoretical predictions, i.e., trim magnification can either be increased or decreased near resonance depending on the sign and magnitude of J_{YZ}. Because of the large rapid variations in λ which occurred as δ_{YZ} was increased, no explosive divergences in trim angle were observed in the 6-DOF results; however, conditions of persistent resonance were observed at high altitudes. The mechanism for these highly oscillatory conditions of persistent resonance is described by the quasi-steady trim angle relations and Eq. (5). It can be concluded from the results presented herein that near resonance, when trim producing asymmetries are present, physically realizable values of the transverse product of inertia can cause changes in the trim magnification and roll rate behavior displayed by slender re-entry vehicles.

References

[1] Hodapp, A. E., Jr., "Effects of Unsymmetrical Stability Derivative Characteristics on Re-Entry Vehicle Trim Angle Behavior," *Journal of Spacecraft and Rockets*, Vol. 11, No. 5, May 1974, pp. 300–307.

[2] Hodapp, A. E., Jr. and Clark, E. L., Jr., "Effects of Products of Inertia on Re-Entry Vehicle Roll Behavior," *Journal of Spacecraft and Rockets*, Vol. 8, No. 2, Feb. 1971, pp. 155–161.